Square Wave Anodic Stripping Voltammetry at the Mercury Film Electrode: Theoretical Treatment

S. P. Kounaves, J. J. O'Dea, P. Chandresekhar,[1] and Janet Osteryoung*

Department of Chemistry, State University of New York at Buffalo, Buffalo, New York 14214

The theoretical treatment of square wave anodic stripping voltammetry at a mercury film electrode is presented. Numerical calculations, using the step method, show that the differential current voltammograms are symmetrical and the peak potential, E_p, shifts to more negative potentials ($\partial nE_p/\partial \log \Lambda = 59.2$ mV) with decreasing film thickness parameter $\Lambda = l/(D_R\tau)^{1/2}$. For $\Lambda < 0.3$, peak current is proportional only to square wave (SW) frequency (f) and amount of metal deposited in the mercury layer (q_R) and gives a response 6 times as great as other stripping waveforms ($\Delta I_p = 0.298nq_Rf$ under typical conditions with a 50-mV SW amplitude, a 10-mV step height, and $n = 1$). The peak width changes from a constant 124 mV for $\Lambda > 3$ to 99 mV for $\Lambda < 0.3$.

In a previous paper (*1*) we presented the theory and numerical calculations for square wave voltammetry (SWV) at the mercury film electrode (MFE) for reversible reduction of metal ion to amalgam. In this paper we derive the theory and present numerical calculations for the current–potential curves obtained during an oxidizing square wave scan for an anodic stripoping voltammetry (ASV) experiment, also at the MFE. A general description of SWV can be found in the literature (*2*).

ASV itself is an attractive technique for rapid and sensitive determination of trace metals in solution. Pulse methods of ASV possess an advantage over linear scan ASV (LSASV) in that they discriminate effectively against charging current (*3*). Differential pulse ASV (DPASV) with the normally used scan rate range of 2–10 mV/s gives rise to unnecessarily long stripping times (ca. 500 s/V) when compared with the short deposition times (<200 s) obtainable at the MFE. While staircase ASV (SCASV) does not have this problem, it is inferior to LSASV in terms of sensitivity and to DPASV in terms of discrimination against background currents. With a fairly customary SWV scan rate of ca. 5 V/s, a 1-V range can be scanned in 200 ms, whereas comparable scan times with LSASV (20 s) or DPASV (500 s) are substantially greater.

Among all of the pulsed ASV methods, ASV utilizing a square-wave waveform (SWASV) appears to combine the best features of these methods. It offers a method having a short analysis time and in addition equals or surpasses the other pulse techniques in sensitivity and discrimination against charging current background. Its utility has been demonstrated experimentally in conjunction with the stationary mercury drop electrode (*4*) and the wall-jet MFE (*5*).

THEORY

The treatment given here for SWASV at the MFE is an extension of those given earlier for staircase ASV (SCASV) (*6*) and square wave direct voltammetry (SWDV) (*1*). The reader is referred to the latter paper for more detail than the following condensed version provides.

[1]Present address: Physical Sciences Center, Honeywell, Inc., Bloomington, MN 55420-5601.

We consider an ASV experiment using a MFE of thickness l into which a metal M has been reduced such that its initial and homogeneous concentration is C_R^*, corresponding to a total charge of $q_R = nFAlC_R^*$, the other symbols having their usual meaning. We also assume that Fick's laws of diffusion apply to both reduced the oxidized forms of the metal and that the reaction

$$M(Hg) = M^{n+} + ne^- \quad (1)$$

is reversible. However, the boundary conditions are slightly altered from the SWDV case (*1*) to reflect the starting condition of a homogeneous bulk concentration C_R^* inside the restricted diffusion layer (Hg). We thus have

$$C_R(x,0) = C_R^* \qquad l \geq x \geq 0 \quad (2)$$

$$C_O(y,0) = 0 \qquad y \geq 0 \quad (3)$$

$$C_O(y<0,t\geq 0) = 0 \quad (4)$$

The concentrations of C_R and C_O can be expressed by the integral equations (*1*, *6*)

$$C_O(0,t) = (1/nFA(\pi D_O)^{1/2}) \int_0^t (i(u)/(t-u)^{1/2})\, du \quad (5)$$

$$C_R(0,t) = C_R^* - (1/nFA(\pi D_R)^{1/2}) \int_0^t (i(u)H_3(a)/(t-u)^{1/2})\, du \quad (6)$$

where $a = [D_R(t-u)]^{1/2}/l$, D_R and D_O are the diffusion coefficients of M in the Hg and M^{n+} in the solution, respectively, and H_3 is an eta function (*1*). Combination of eq 5 and 6 with the Nernst equation

$$D_O^{1/2}C_O(0,t) = \epsilon D_R^{1/2}C_R(0,t) \quad (7)$$

where $\epsilon = \exp[nf(E - E_{1/2})]$, $E_{1/2}$ is the reversible half-wave potential, and $f = F/RT = 38.92$ V^{-1} at 25 °C, results in

$$\frac{1}{\epsilon}\int_0^t (i(u)/(t-u)^{1/2})\, du + \int_0^t (i(u)H_3(a)/(t-u)^{1/2})\, du = nFA(\pi D_R)^{1/2}C_R^* \quad (8)$$

We make this equation dimensionless by defining the quantities

$$\psi(t) = i(t)(\pi\tau)^{1/2}/nFAD_R^{1/2}C_R^* \quad (9)$$

$$z = t/\tau \quad (10)$$

$$\xi = u/\tau \quad (11)$$

resulting in

$$\frac{1}{\epsilon}\int_0^z (\psi(\xi)/y^{1/2})\, d\xi + \int_0^z (\psi(\xi)H_3(y^{1/2}/\Lambda)/y^{1/2})\, d\xi = \pi \quad (12)$$

where $y = z - \xi$ and $\Lambda = l/(D_R\tau)^{1/2}$ (the dimensionless thickness parameter).

As in the previous paper (*1*) eq 12 was converted to numerical form using the step-method and translated into a

0003-2700/87/0359-0386$01.50/0

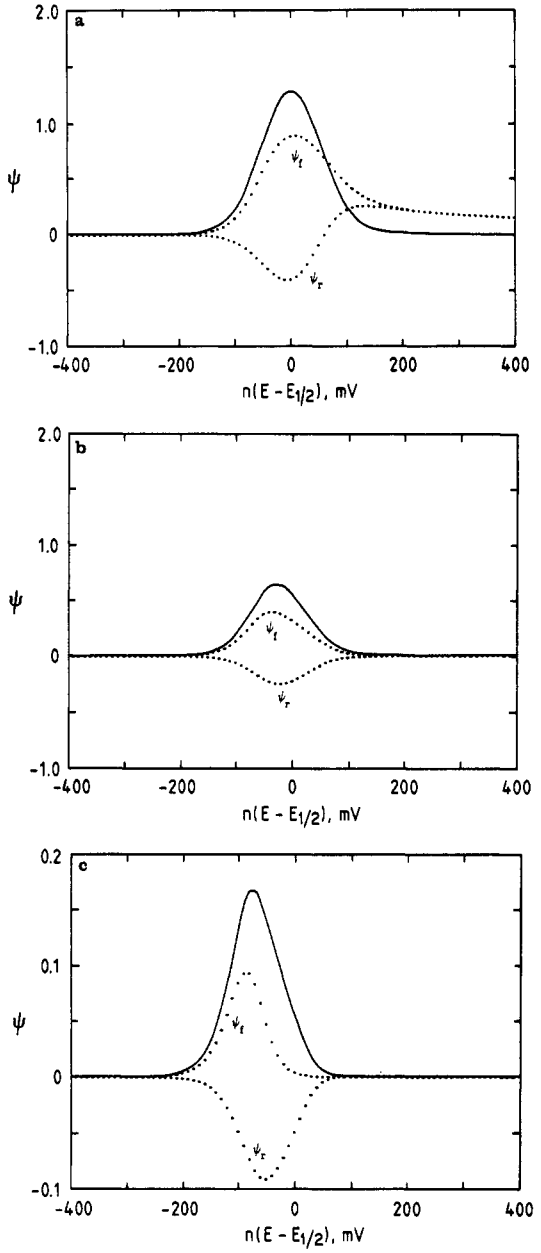

Figure 1. Calculated current function stripping voltammograms for forward (f) and reverse (r) (both •••) and net (——) current for Λ equal to (a) 30, (b) 1.0, and (c) 0.3, where $\Lambda = l/(D_R\tau)^{1/2}$, $n\Delta E_s$ = 10 mV, and nE_{sw} = 50 mV.

FORTRAN IV program for calculation of the dimensionless current function ψ as a function of $n(E - E_{1/2})$ for various values of Λ.

Peak heights and positions were determined from the vertex of the parabolic fit to the three largest dimensionless currents of the voltammogram. Peak widths were defined by tangents to the voltammogram at half-height. The differential current function, $\Delta\psi$, corresponds to the difference between forward and reverse currents and $\Delta\psi_p$, to the peak current.

RESULTS AND DISCUSSION

Representative results of the numerical calculations are shown in Figure 1. for the three different values of Λ, using step height $n\Delta E_s$ = 10 mV and square wave amplitude nE_{sw} = 50 mV, the net current ($\Delta\psi$) stripping voltammogram retains its symmetrical shape even though the reverse and forward peaks change shape noticeably depending on the value of Λ (7). The effect of changing Λ on the peak height ($\Delta\psi_p$), peak position $n(E_p - E_{1/2})$, and peak width ($nW_{1/2}$), is better shown in Figures 2–4, respectively.

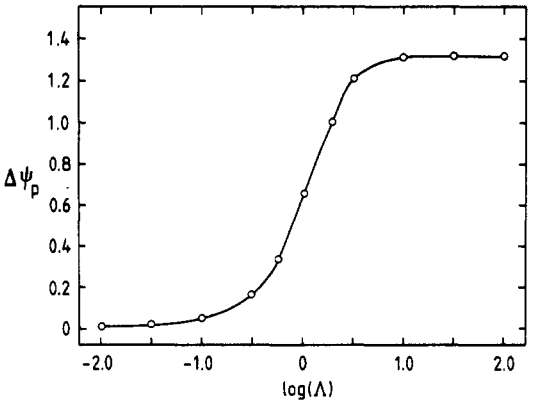

Figure 2. Dependence of the current-function peak height, $\Delta\psi_p$, on log Λ. $n\Delta E_s$ = 10 mV and nE_{sw} = 50 mV.

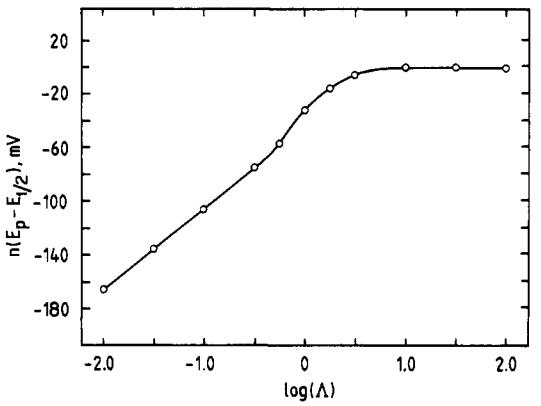

Figure 3. Dependence of the peak potential on log Λ. $n\Delta E_s$ = 10 mV and nE_{sw} = 50 mV.

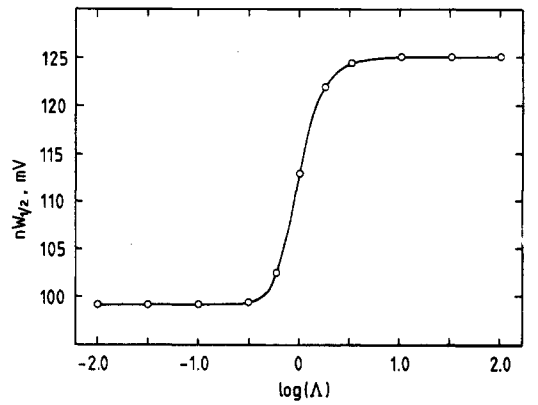

Figure 4. Dependence of the peak width at half height on log Λ. $n\Delta E_s$ = 10 mV and nE_{sw} = 50 mV.

For values of $\Lambda \gg 1$ (unrestricted diffusion in both solution and mercury) all of the peak parameters are constant and identical with those for the net reducing scan of SWV ($\Delta\psi_p$ = 1.312, $nW_{1/2}$ = 124 mV, and $n(E_p - E_{1/2})$ = 0 mV) (1), as is expected.

In contrast to SWDV, for SWASV there is no maximum response for $\Delta\psi_p$ when Λ = 1 (Figure 2), but for $3 \geq \Lambda \geq 0.3$ there is a sudden decrease in $\Delta\psi_p$ indicating the change from unrestricted to restricted diffusion. The same effect is also seen for the peak potential (Figure 3), which changes from a constant value of ca. 0 mV to the Λ-dependent value for restricted diffusion with a slope of 59.2 mV, and for the peak width (Figure 4), which changes from a constant value of 124 mV to a constant value of 99 mV.

Limiting Case for $\Lambda \rightarrow 0$. The case when $\Lambda \ll 0.3$ deserves special consideration. In this situation the diffusion within the Hg film appears to be infinitely fast so that no concen-

Table I. Effect of Square Wave Amplitude, nE_{sw}, on Voltammogram Characteristics ($n\Delta E_s$ = 10 mV, Λ = 0.01)

nE_{sw}, mV	$n(E_p - E_{1/2})$, mV	$nW_{1/2}$, mV	$10^3\Delta\psi_p$
1	−132	66	0.632
5	−137	70	1.314
10	−140	72	2.138
20	−144	75	3.523
50	−165	99	5.283
80	−193	124	5.522
100	−213	132	5.544

tration gradients develop on the time scale of the potential-step perturbation ($\tau/2$) and C_R* is fixed by the ratio of the surface concentrations. In this thin-film case (achieved in practice by sufficiently small values of either the Hg-film thickness (l) or the SW frequency (f)), as $\Lambda \rightarrow 0$, $H_3(a) \approx a\pi^{1/2}$. Thus, eq 12 can be simplified and solved numerically, yielding a linear dependence of $\Delta\psi_p$ on Λ. For $\Lambda < 0.1$

$$\Delta\psi_p = 0.298\pi^{1/2}\Lambda = 0.528\Lambda \quad (13)$$

Combining eq 9, eq 13, all constants, and recalling that $\Lambda = l/(D_R\tau)^{1/2}$ where $\tau = 1/f$, we obtain the expression for the experimental differential current at a MFE for $\Lambda < 0.1$

$$\Delta i_p = (2.874 \times 10^4)nAC_R^*lf \quad (14)$$

Since in ASV the initial conditions are almost always coulometric, that is, $q_R = i_d t_d = nFAC_R^* l$, we then have

$$\Delta i_p = 0.298nq_Rf = 0.298ni_dt_df \quad (15)$$

where i_d and t_d are the (constant) current and time during the deposition step. In addition we also have at Δi_p for $\Lambda < 0.1$

$$n(E_p - E_{1/2}) = -46.7 + 59.2 \log \Lambda, \text{ mV} \quad (16)$$

and

$$nW_{1/2} = 99.2 \text{ mV} \quad (17)$$

These results are analogous to those for linear scan ASV (*8*, *9*) at the MFE. The dimensionless peak current $\Delta\psi_p$ depends on Λ (eq 13), and the peak potential shifts to more negative values with decreasing Λ, with a slope $\partial nE_p/\partial \log \Lambda = 59.2$ mV (eq 16). Under coulometric conditions for the deposition, eq 15 applies, and the measured peak current is proportional, through i_d, to the initial concentration of M^{n+}, but independent of l. This feature obtains regardless of the choice of voltammetric waveform and makes ASV at the MFE a feasible analytical technique.

The effects of varying the square wave amplitude, nE_{sw}, on the stripping parameters (for $\Lambda = 0.01$), are summarized in Table I. The behavior is qualitatively the same as that for unrestricted diffusion and for SWDV (*1*). The peak shifts to more negative values and increases in height with increasing amplitude. For $nE_{sw} < 10$ mV the reverse pulses are not sufficiently large to re-reduce the metal, and as $nE_{sw} \rightarrow 0$, $\Delta\psi \rightarrow 0$ as $\psi_f \rightarrow \psi_r$, so that a plot of $\psi_f + \psi_r$ gives a peak identical with that for the SCASV experiment (*6*). For $nE_{sw} \geq 50$ mV the pulses span the peak, which causes the positive side of the reverse-current (cathodic) peak (ψ_r) to become enlongated, which in turn distorts the positive side of the differential-current peak ($\Delta\psi$). From a plot of the theoretical values of $\Delta\psi_p/nW_{1/2}$ vs. nE_{sw}, the optimum value of nE_{sw} occurs at ca. 36–40 mV.

Changes in the step height, $n\Delta E_s$, do not affect strongly the peak parameters. For $\Lambda = 0.01$ and $nE_{sw} = 50$ mV, increasing $n\Delta E_s$ from 10 to 30 mV changes the peak position from −165 to −158 mV with respect to $E_{1/2}$, the peak width from 99 to 86 mV, and the peak current function from 5.3×10^{-3} to 6.6×10^{-3}.

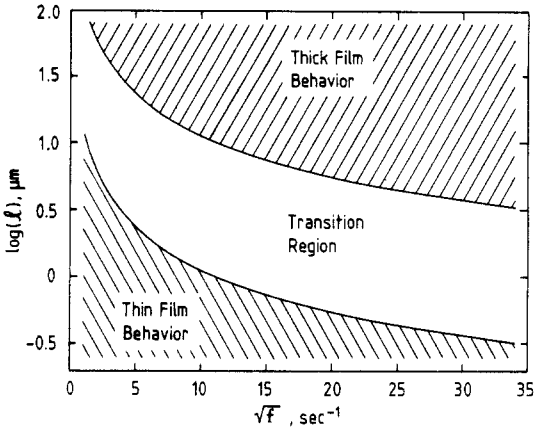

Figure 5. Types of behavior expected for typical values used in SWASV, $D_R = 1.5 \times 10^{-5}$ cm²/s, $nE_{sw} = 50$ mV, and $n\Delta E_s = 10$ mV.

Table II. Comparison of the Theoretical Faradaic Current Response for Different Voltammetric Waveforms Used in ASV under Typical Conditions

technique	time parameter	characteristic time, t_c	i_p/nq_R, s^{-1}	i_pt_c/nq_R
LSASV[a]	ν = 1 V/s	$RT/nF\nu$	11.6	0.30
SCASV[b]	f = 200 Hz	$1/f$	11.2	0.06
DPASV[c]	t_p = 12 ms	t_p	11.5	0.14
SWASV[d]	f = 200 Hz	$1/2f$	60.0	0.30

[a] Reference 9. [b] Step height = 10 mV; equivalent scan rate = 2 V/s; ref 6. [c] In the limit of large amplitude for which DPASV approaches normal pulse ASV; ref 10. [d] $n\Delta E_s$ = 10 mV; nE_{sw} = 50 mV; equivalent scan rate = 2 V/s.

Earlier experimental work supports the results presented here (*11*); also we are carrying out a more thorough experimental investigation for future publication.

In addition to predicting the morphology and values of parameters of the stripping peaks, the above numerical results suggest specific ranges of Λ within which thin-film, thick-film, or transitional behavior may be observed. Figure 5 shows the behavior expected for typical values of l and f, with values of $D_R = 1.5 \times 10^{-5}$ cm²/s, $nE_{sw} = 50$ mV, and $n\Delta E_s = 10$ mV. For example, with the commonly used SW frequency of 60 Hz, thin film behavior is attained for Hg films of less than 1 μm thickness. For the same frequency the range 1 μm < l < 15 μm is a transition region where small changes in l can cause large changes in $\Delta\psi_p$.

Finally, we compare the theoretical sensitivity of SWASV with that of other stripping techniques. In each case the peak current is given by

$$i_p = nq_R\psi_p/t_c \quad (18)$$

where t_c is the characteristic time of the voltammetric technique and ψ_p is the dimensionless peak current. Normally sensitivity is defined as the slope of a (linear) calibration curve. In this case q_R, which depends on both concentration and the parameters of the deposition step, is used as a surrogate for concentration, and thus the sensitivity is given by $i_p/nq_R = \psi_p/t_c$ (Table II). Since most voltammetric techniques can be used, at least in principle, over a wide range of characteristic time, it is useful also to compare the values $i_pt_c/nq_R = \psi_p$, also shown in Table II. Under typical conditions, for which each technique performs reliably yet gives a good response, SWASV is about 6 times as sensitive as the other techniques. The dimensionless sensitivity, ψ_p, does not differ markedly for the various techniques, so it is easy to make one technique appear the most sensitive by appropriate choices of t_c. It is more reasonable to view these techniques as being comparable in

sensitivity. Furthermore, sensitivity is not typically the limiting factor in applications of ASV at mercury film electrodes.

ACKNOWLEDGMENT

The authors wish to thank Mary Schreiner for her valuable comments and helpful suggestions.

LITERATURE CITED

(1) Kounaves, S. P.; O'Dea, J. J.; Chandresekhar, P. C.; Osteryoung, J.; *Anal. Chem.* **1986**, *58*, 3199-3202.
(2) Osteryoung, J.; Osteryoung, R. A. *Anal. Chem.* **1985**, *57*, 101A-110A.
(3) Copeland, T. R.; Christie, J. H.; Osteryoung, R. A.; Skogerboe, R. K. *Anal. Chem.* **1973**, *45*, 2171-2174.
(4) Wojciechowski, M.; Go, W.; Osteryoung, J. *Anal. Chem.* **1985**, *57*, 155-158.
(5) Wechter, C.; Sleszynski, N.; O'Dea, J.; Osteryoung, J. *Anal. Chim. Acta* **1985**, *175*, 45-53.
(6) Christie, J. H.; Osteryoung, R. A. *Anal. Chem.* **1976**, *48*, 869-872.
(7) Aoki, K.; Tokuda, K.; Matsuda, H.; Osteryoung, Janet *J. Electroanal. Chem.* **1986**, *207*, 25-39.
(8) de Vries, W. T. *J. Electroanal. Chem.* **1965**, *9*, 448-456.
(9) de Vries, W. T.; van Dalen, E. *J. Electroanal. Chem.* **1967**, *14*, 315-327.
(10) Osteryoung, R. A.; Christie, J. H. *Anal. Chem.* **1974**, *46*, 351-355.
(11) Turner, J. A.; Eisner, U.; Osteryoung, R. A. *Anal. Chim. Acta* **1977**, *90*, 25-34.

RECEIVED for review July 18, 1986. Accepted October 1, 1986. This work was supported in part by the National Science Foundation under Grant Numbers CHE 8305748 and 8521200.

Iridium-Based Small Mercury Electrodes

Janusz Golas,[1] Zbigniew Galus,[2] and Janet Osteryoung*

Department of Chemistry, State University of New York at Buffalo, Buffalo, New York 14214

A method of the preparation of small (63.5 μm radius, ~60 μm thick) mercury electrodes based on an iridium disk support is described. The electrodes are of hemispherical shape and are relatively durable, and the potential range for their use overlaps with that for hanging mercury drop electrodes. In situ microscopic observations combined with electrochemical measurements indicate that the amount of mercury required to attain complete coverage is equivalent to ~50% of that required to form a regular hemisphere of the radius of the iridium base. The most durable electrodes were those with the amount of deposited mercury sufficient to form such a regular hemisphere. Some cyclic linear scan and stripping experiments are described to present the behavior of this type of electrode.

Mercury electrodes have a central role in developments in electroanalytical chemistry because of the reproducibility of the mercury surface. Commonly used implementations include the dropping mercury electrode (DME), the hanging drop (HMDE) (*1*), various automated hanging drop electrodes such as those developed by EG&G PARC and by Metrohm, and the film electrode (*2*). These electrodes are used for direct voltammetry and, with the exception of the DME, for anodic stripping voltammetry. The hanging drop-types of electrodes have mechanical difficulties associated with the intrinsic problem of handling liquid mercury. On the other hand, so-called film electrodes are generally inhomogeneous (*3*). But the idea of preparing a mercury electrode by cathodic reduction of mercury at a foreign substrate is attractive, for it provides the possibility of making electrodes in a range of sizes without mechanical problems and avoiding handling bulk mercury.

A support material for mercury films should be easily wetted by mercury, but on the other hand its solubility in mercury should be very low. Practically it is almost impossible to combine these two features. Films deposited on supports of platinum, silver, gold, or nickel exhibit a reasonably uniform surface due to good wetting, but solubility of these metals in mercury cannot be neglected. The formation of intermetallic compounds of a metal deposited into the film with a base material then must be taken into account. In the case of glassy carbon used as a support, one faces different problems. Carbon is chemically inert but the mercury deposit does not wet the substrate and thus forms a collection of droplets, making the surface inhomogeneous (*3*). In spite of problems arising from this inhomogeneity, mercury-film electrodes have found wide electroanalytical application (*4*).

The possibility of deposition of mercury on a large iridium disk has been reported recently by Kounaves and Buffle (*5*, *6*). This base material seems to exhibit very good properties of two kinds: first, its solubility in mercury is very low (below 10^{-6} wt %) (*7*); second, mercury can be electroplated onto the iridium in such a way that it wets the surface. Although the procedure proposed for preparing a film on a large disk was a bit complicated (mechanical, chemical, and electrochemical pretreatments were required), it resulted in uniform and stable mercury films.

There are several recent reports on deposition of mercury on substrates of different shapes and materials (*8-11*). The most recent report on mercury microvoltammetric electrodes was by Wehmeyer and Wightman (*8*). The bases for their hemispherical mercury electrodes were platinum disks of 10, 2, and 0.6 μm diameter. Although it was shown that mercury can be relatively easily deposited on a Pt microdisk, still the problem of interaction of mercury and platinum, especially at longer times, remains. Despite this, it should be emphasized that a practical very small mercury electrode opens to study fundamental problems in electrochemistry for which only mercury electrodes are suited and also broadens and strengthens practical analytical applications. We report in this paper investigations on the use of a small iridium disk (127 μm diameter) as a base for small mercury electrodes.

EXPERIMENTAL SECTION

Instrumentation. The measuring system consisted of an RDE 3 Model potentiostat (Pine Instrument Co.) and Houston In-

[1] Permanent address: Academy of Mining and Metallurgy, Institute of Material Sciences, Al. Mickiewicz 30, 30-059 Cracow, Poland.
[2] Permanent address: University of Warsaw, Department of Chemistry, Pasteur 1, 02-093 Warsaw, Poland.

0003-2700/87/0359-0389$01.50/0